

Oxidation induction time and oxidation onset temperature of polyethylene in air

Testing Gimzewski's postulate

Walter W. Focke¹ and Isbe van der Westhuizen¹

(1) Institute of Applied Materials, Departments of Chemistry and of Chemical Engineering, University of Pretoria, Pretoria, 0002, South Africa

Corresponding author: Walter W. Focke
Email: walter.focke@up.ac.za

Abstract

Oxidation induction times (OIT) and oxidation onset temperatures (OOT) of a low density polyethylene melt were evaluated in air using DSC. Good regression fits to OOT data were obtained using global values for the activation energy (E) that are specific for each antioxidant but assumed independent of concentration. Gimzewski's postulate that OIT and OOT correspond to the same level of antioxidant depletion was tested by attempting to predict OIT values from OOT generated model parameters. The deviations between predicted and experimental OIT values were comparable in magnitude to the inherent scatter in the data. However, regression of the dynamic OOT data yielded statistically significant lower values for the activation energy than are obtained by direct regression of isothermal data.

Keywords: Accelerated ageing - Antioxidant - Oxidation induction time - Polyethylene

Introduction

Organic polymers are subject to degradation by atmospheric oxygen even at ambient conditions. According to the widely accepted mechanistic model proposed by Bolland and Gee [1] such hydrocarbon oxidation proceeds as an autocatalytic, free radical chain reaction process. The repeating sequence of steps involves free radical initiation, propagation, chain branching and termination reactions. At the molecular level, new functional groups such as aldehydes, alcohols, esters, hydroperoxides, ketones, etc., are introduced. The polymer also suffers structural changes owing to branching, crosslinking and chain scission reactions [2]. Macroscopic observable effects vary from simple discoloration, through a reduction in gloss, to embrittlement and cracking. Eventually complete loss of mechanical integrity results.

Antioxidants are used to retard polymer oxidation and to minimize the associated damage [3]. They act by interrupting the degradation cycle and are generally consumed during the stabilization process. The technical literature distinguishes between primary and secondary antioxidants [4]. Primary antioxidants (HA) are hydrogen donors that function by a chain breaking donor mechanism that terminates the propagation reaction. Hindered phenols are an example of this type. However, they also permit the chain initiating hydroperoxide to be regenerated. Secondary antioxidants (D) decompose hydroperoxides to non-radical products.

The protection offered by antioxidants at a specified fixed temperature is characterized by an induction period [5–7]. During this induction period polymer degradation is inhibited while the antioxidants are consumed. Thus stability is determined by the residual level of antioxidant remaining in the material [8]. Once the antioxidant level dips below a critical value, catastrophic polymer degradation commences.

The oxidative stability of organic materials containing antioxidants may be assessed directly using thermal analysis. Suitable methods include oven ageing, differential scanning calorimetry (DSC), differential thermal analysis, thermogravimetric analysis, chemiluminescence, etc. [9, 10] The results of such studies are of value for two main reasons: They can provide indications of residual life-time or provide estimates of the concentration of active antioxidant remaining in the material [11–15]. Two main DSC-based methods are used in industry as accelerated-oxidation quality control techniques [6, 16]. The distinction is between DSC experiments run under isothermal conditions to give an oxidation induction time (OIT) [5], and those conducted at a constant temperature scan rate to give an oxidation onset temperature (OOT) [6, 17]. The principles of these two methods are as follows: The OIT is the time (t_{iso}) that elapses before the sample exhibits a sudden exothermic oxidation reaction in an isothermal experiment. OOT corresponds to the onset temperature (T_{onset}) of this exotherm as observed in a temperature scanning experiment.

It has been asserted that OIT has limited value for estimating polymer service life [9]. Nevertheless, the OIT technique is a well established quality control method described in ASTM (e.g. ASTM D 3895-02) and ISO (e.g. ISO 11357-6) standards [16]. The isothermal mode requires a priory selection of a suitable temperature. It may be prescribed by the quality control test. However, if this is not the case, the selection of a suitable temperature can be problematic. When chosen at too low or too high temperatures the induction times will either be impractically long or too short, respectively [6]. In the latter case the precision of the measurement may be compromised by the finite time required to switch between the inert and oxidative gases. Errors introduced by the switching between gases are not a problem when using the scanning mode. Recent round robin tests [16] indicate that OIT determination, especially of low values, is associated with a high degree of uncertainty. It was suggested that OOT could provide a viable alternative in such instances. It is interesting to note that a reference material, with well-defined OIT and OOT values, is commercially available [18].

Ideally there should be a definitive relationship linking OOT and OIT. Goh [19, 20] proposed the construction of such a mastercurve via shift factors based on the peak temperatures obtained in dynamic scans. Gimzewski [6] used a simple kinetic model to link these two methods. He argued that the relationship between OIT and OOT has both theoretical and practical significance. For example, time-wasting trial-and-error OIT measurements can be avoided if dynamic temperature scans can be used to determine a suitable temperature for the isothermal run.

Figure 1 shows a plot of paired OIT–OOT values obtained for stabilized polyethylene reported by Schmid et al. [16]. Figure 2 compares experimental OIT data [21] with predictions from OOT evaluations. In both cases the data reduction used a common activation energy as suggested by Gimzewski [6]. This initial check, using limited literature data, revealed that his approach holds promise. This prompted us to re-explore the relationship between OIT and OOT via a

modification of Gimzewski's simple empirical model. In this communication we present revised analytic expressions that are based on a temperature integral approximation due to Madhusudanan et al. [22]. These expressions were then used to analyze OOT and OIT experimental data for three different antioxidants at different concentrations in low density polyethylene.

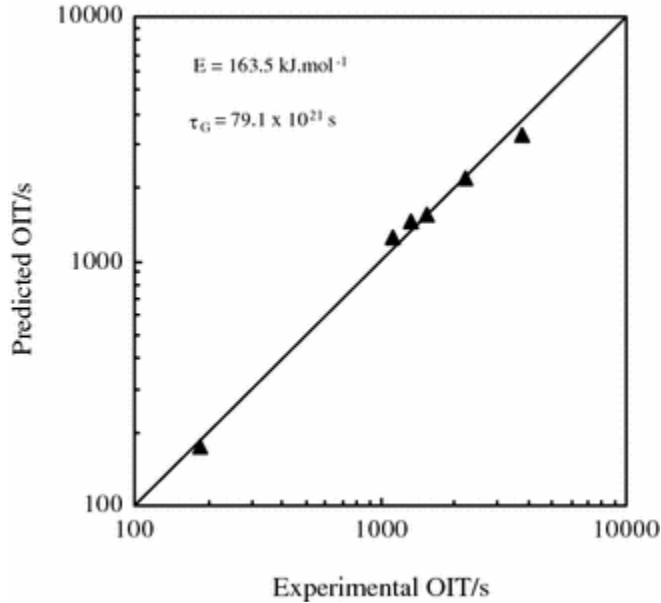


Fig. 1 Test of Gimzewski's [6] "universal" activation energy postulate by fitting Eq. 23 to the data set of paired OIT–OOT values published by Schmid et al. [16] for polyethylene oxidation

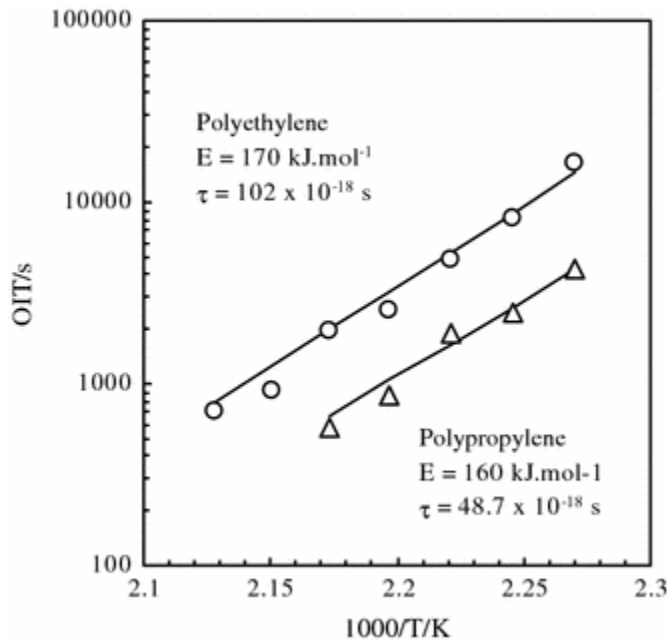


Fig. 2 Predicting OIT values from OOT evaluations using data of Šimon [21]. Symbols represent OIT experimental points and solid lines predictions generated from the OOT data

Oxidation induction time/onset temperature: Kinetic modeling

Most solid–gas or liquid–gas reactions, e.g. the oxidation of a polymer, occur via multiple primitive reaction steps, each with their own characteristic temperature-dependent rate constant [23, 24]. In addition, diffusion and migration effects may play a role [25]. Despite these complications, Colin et al. [26] succeeded in employing such a fundamental set of differential equations to predict the oxidation of an unstabilized polyethylene. However, more often the exact mechanisms are unknown or too complicated to be tractable [21, 27]. Malík and Kröhnke [4] declare: “Present theoretical understanding of polymer degradation and stabilization principles does not yet sufficiently cover the full chemical and physical complexity of polymer stabilization ...” Thus, for simplicity and convenience such systems are frequently modeled using the so-called single step reaction approximation [21, 27]. It is assumed that the process can be described by an (apparent) first order differential equation analogous to the kinetic expression for a single homogeneous chemical reaction [28]. Obviously such an equation would in fact apply when the overall kinetics is chemically controlled by a single primitive reaction, e.g. antioxidant consumption during the induction period [8].

$$\frac{d\alpha}{dt} = k(T) f(\alpha) \quad (1)$$

Here α is a dimensionless degree of conversion, k is the reaction rate constant, and $f(\alpha)$ is a depletion function applicable to the rate limiting reaction. As is customary, Arrhenius-type temperature dependence is assumed for the rate constant k [29]:

$$k = k_0 e^{-E/RT} \quad (2)$$

Gimzewski [6] assumed that direct oxidation of the hydrocarbon is the rate limiting reaction. He constructed a link between the isothermal induction times and dynamic onset temperatures by positing that the observed OIT and OOT values correspond to equivalent critical values of hydrocarbon conversion α_{crit} . He further suggested that this state only depends on the nature of the antioxidants and their initial concentrations. This expectation has some justification considering that oxidative attack on the polymer leads to antioxidant depletion. The Gimzewski assumptions essentially transform OOT and OIT analyses to the solution of classic model-free isoconversion thermal analysis problems. These were recently reviewed by Starink [30]. The Gimzewski postulate implies an activation energy that is substrate dependent but independent of the nature of the antioxidant.

Instead we put forward the notion that consumption of the oxidation inhibitors constitutes the limiting reaction. The data presented by Shlyapnikov et al. [8] provides support for this assertion. It clearly shows that the induction period ends at the point where the antioxidant level becomes negligible. Our revised interpretation implies that the activation energy could vary with the nature of the antioxidant. In this framework the link between OOT and OIT is also different: Both refer to equivalent critical residual concentrations of the antioxidants rather than a fixed conversion. This means that the critical conversion is not constant but that it varies with the initial antioxidant concentration:

$$\alpha_{\text{crit}} = 1 - C_{\text{crit}}/C_o \quad (3)$$

It is nevertheless convenient to assume that the end of the induction period corresponds to complete depletion of the antioxidants in which case $\alpha_{\text{crit}} \approx 1$. This is permissible except when the antioxidant depletion follows first order kinetics.

An important feature of Eq. 1 is that the rate is proportional to the product of separate functions of temperature and conversion. This allows the differential equation to be solved by the method of separation of variables:

$$\tau \equiv \frac{1}{k_o} \int_0^{\alpha_{\text{crit}}} \frac{d\alpha}{f(\alpha)} = \int_0^{t_{\text{onset}}} e^{-E/RT} dt \quad (4)$$

Here τ is a characteristic time constant of the ersatz chemical reaction determining the length of the induction time period t_{onset} . The latter corresponds to the time where the antioxidant depletion attains the critical concentration. It is important to recognize that at that point the integral on the right is also invariant and equal to the time constant τ . It is also taken for granted that $\alpha_{\text{crit}} \approx 1$ in Eq. 4 or otherwise that it is defined by Eq. 3.

The isothermal case represents the simplest situation for kinetic evaluations as integration of the right hand in Eq. 4 becomes facile. The solution is:

$$t_{\text{iso}} = \tau e^{E/RT_{\text{iso}}} \quad (5)$$

Thus, provided the assumptions stated above apply, Eq. 5 predicts that a plot of the logarithm of the oxidation induction time (OIT = t_{iso}) against the reciprocal of the absolute isothermal temperature should yield a straight line with slope E/R .

If the antioxidant depletion reaction follows n th order kinetics, and the critical antioxidant concentration is zero, the time constant is given by:

$$\tau = \frac{C_o^{1-n}}{(1-n)k'_o} \quad (6)$$

With first order behavior the governing relationship is:

$$\tau = \frac{1}{k_o} \ln \frac{C_o}{C_{\text{crit}}} \quad (7)$$

Gimzewski [6] examined the experimental difficulties associated with the execution of precise isothermal experiments with gas-solid reactions. He states that it is easier to control experimental conditions (e.g. gas atmosphere and gas flow rate) using temperature-programmed thermal analysis with linear temperature ramping:

$$T(t) = T_0 + \beta t \quad (8)$$

Substituting Eq. 8 into Eq. 4 and simplifying yields the following integral forms:

$$\tau = \frac{1}{k_o} \int_0^{\alpha_{crit}} \frac{d\alpha}{f(\alpha)} = \frac{1}{\beta} \int_0^{T_{onset}} e^{-E/RT} dT \quad (9)$$

The choice for the lower integration limit in the integral on the right is justified by the fact that the dynamic scan experiment should start at a temperature that is low enough for the effective reaction rate to be negligible. The temperature integral can be transformed into a more convenient form by changing variables making use of

$$x = E/RT \quad (10)$$

Then

$$\frac{R}{E} \int_0^{T_{onset}} e^{-E/RT} dT = \int_{\infty}^{x_{onset}} \frac{e^{-x}}{x^2} dx \equiv p(x_{onset}) \quad (11)$$

Equating Eqs. 5 and 9 at the corresponding induction and onset points, and substituting 11, yields the following dimensionless link between OIT (t_{iso}) and OOT (T_{onset}):

$$\frac{p(x_{onset})E}{\tau \beta R} = \frac{t_{iso}}{\tau} e^{-E/RT_{iso}} = 1 \quad (12)$$

Note that the pre-exponential factor of the Arrhenius rate constant (k_o) does not appear explicitly in this relationship. For dynamic data, solving Eq. 12 requires evaluation of the temperature integral $p(x)$. Previous OIT studies used numerical techniques for this purpose [6, 7, 15]. However, we will show that a tractable analytic expression is possible.

Starink [30] and Flynn [31] critically reviewed various published procedures for evaluating the temperature integral. Ji [32] developed very accurate rational approximations. Focke et al. [33] proposed the following approximation valid for $x > 10$:

$$-\ln p(x) = x + \ln x - \ln \left(\frac{x + 3}{x^2 + 5x + 4} \right) \quad (13)$$

However, Madhusudanan et al. [22] proposed a particularly useful class of approximations which, as we shall show, is more suitable for rapid and convenient evaluation of the activation energy:

$$-\ln p(x) = a + bx + c \ln x \quad (14)$$

Substituting Eq. 14 in Eq. 12 and simplifying yields a straight line expression in the reciprocal temperature [30]:

$$\ln (\beta/T^c) = K - bE/RT \quad (15)$$

with intercept $K = (1 - c) \ln (E/R) - a - \ln \tau$ and slope $-bE/R$. Equation 15 shows that the approximation proposed by Madhusudanan et al. [22] allows determination of the activation energy using simple linear regression. The classic Kissinger–Akahira–Sunose (KAS) and Flynn–Wall–Ozawa (FWO) methods are special cases of Eq. 15. They are obtained by assigning the proper values to the constants a , b and c [30]. Starink [30] states that $15 < x < 60$ holds for the overwhelming majority of reactions. The revised values for the constants published by Tang et al. [34] provide acceptable accuracy in this range:

$$a = 0.37773896; b = 1.00145033 \text{ and } c = 1.89466100 \quad (16)$$

An explicit expression for the activation energy from two dynamic data points

Next we derive an explicit expression for the activation energy using data from dynamic measurements done at two different scan rates [35]. Taking natural logarithms, Eq. 12 can be combined with Eq. 14 and written as

$$\ln \beta - \ln p(x_{\text{onset}}) = \ln (E/\tau R) = \text{constant} \quad (17)$$

For clarity purposes we drop the subscripts “onset” and “iso” from here on. Consider two OOT measurements obtained at different scan rates

$$\ln \beta_2 - \ln p(x_2) = \ln \beta_2 + a + b x_2 + c \ln x_2 \quad (18)$$

$$\ln \beta_1 - \ln p(x_1) = \ln \beta_1 + a + b x_1 + c \ln x_1 \quad (19)$$

According to Eq. 17, the left hand sides of Eqs. 15 and 16 are identical. Equating and simplifying yields the following direct estimate for the activation energy:

$$E = \frac{R T_1 T_2}{b(T_1 - T_2)} \ln \left[\frac{\beta_1}{\beta_2} \left(\frac{T_2}{T_1} \right)^c \right] \quad (20)$$

Once a convenient OIT time period is selected, the temperature that should be considered for the isothermal oxidation experiment run can be calculated from:

$$T_{\text{iso}} = \left[\frac{R}{E} \ln \left(\frac{\beta R t_{\text{iso}}}{E p(x_{\text{onset}})} \right) \right]^{-1} \quad (21)$$

Linking OIT values obtained at a fixed temperature with OOT at a fixed scan rate

Gimzewski [6] original postulate implies that a “universal” activation energy value might be applicable to the oxidation of samples of a similar nature. He suggests a value $E = 140 \pm 30$ kJ/mol for the oxidative stability of lubricating oils. Schmid et al. [16] reported on the oxidative stability measurements for six different samples of polyethylene in an oxygen atmosphere. The OIT values were determined at a temperature of 210 °C and the OOT values at

a scan rate of 10 °C/min. This data permit testing of Gimzewski [6] postulate for polyethylene samples as follows. Equation 12 can be rearranged as follows:

$$\frac{t_{iso}}{p(E/RT_{onset})} = \frac{E}{\beta R} e^{E/RT_{iso}} = \tau_G \quad (22)$$

Since T_{iso} and β are fixed, it follows that the right hand side of Eq. 22 will be invariant provided the notion of a “universal” value for E is actually valid. Thus, for the situation at hand, it was equated to a new time constant τ_G . The link between isothermal and dynamic data is then given by

$$t_{iso} = \tau_G p(E/RT_{onset}) \quad (23)$$

The “best” activation energy E was now associated with the value that minimizes the relative variance of the constant τ_G . This approach is equivalent to minimizing the sum of the relative square errors between predicted and experimental t_{iso} values. Figure 1 shows the encouraging results obtained on regression of the Schmid et al. [16] data in this manner. A value $E = 163.5$ kJ/mol provided the best fit to their data. This is higher than the value obtained for lubricating oils by Gimzewski [6] but it falls inside the uncertainty range that he indicated. The average absolute deviation (AAD) and maximum deviation between predicted and experimental OIT values are 6.8% and 12.7%, respectively. While these results are encouraging, unfortunately, Schmid et al. [16] did not disclose the nature or the concentration of the antioxidants in their samples. It could simply be that the same antioxidant system was employed for all the samples. In that a case common value for E would not be that unexpected.

Predicting OIT from OOT data

Šimon [21] published OIT data for different isothermal temperatures and also OOT values obtained at different scan rates for a polyethylene and a polypropylene sample respectively. The activation energies and the time constant τ were estimated from the dynamic data using Eq. 12. The results are presented in Table 1. The predicted OIT’s are compared to experimentally determined values in Fig. 2. The predictions are, on average, slightly higher than the experimental values determined under isothermal conditions. However, the correspondence between predictions and experimental is acceptable, considering the general uncertainty associated with OIT values as indicated by Schmid et al. [16]. As mentioned in the introduction, these encouraging results obtained on using Gimzewski’s [6] postulate, prompted us to generate additional experimental data to further test its validity.

Table 1 Activation energies, values for the time constant τ and OIT prediction errors for data of Šimon [21]

Polymer	$E/\text{kJ mol}^{-1}$	τ/fs	AAD (%)	Max. error (%)
Polyethylene	170.0	102	16	37
Polypropylene	159.7	487	12	20

Experimental

Low density polyethylene (LDPE) grade LT 019/08 (MFI = 20.5 g/10 min; density = 0.919 g/cm³) supplied by Sasol was used as test resin. It reportedly contains 0.02 wt% of a processing stabilizer based on a proprietary antioxidant blend. Table 2 lists the three different types of antioxidant that were used in this study.

Table 2 Antioxidants properties and suppliers

Antioxidant	Supplier	Type	Chemical name
Anox 20	Great Lakes	Phenolic	Tetrakismethylene (3,5-di-t-butyl-4-hydroxy-hydrocinnamate) methane
Naugard P	Chemtura	Phosphite	Tris(monononylphenyl)phosphite
Orox PK	Orchem	Amine	Polymerized 2,2,4-trimethyl-1,2-dihydroquinoline

Antioxidant masterbatches containing 20 mass% active components were compounded at 20 kg/h on a 40 mm, 42 L/D Berstorff model EV 40 co-rotating twin screw extruder using a flat temperature profile set at 180 °C. These masterbatches were let down to the preselected antioxidant concentrations (0.05, 0.10, 0.20, 0.38 or 0.74 wt%) in the same resin using a 25 mm, 30 L/D Rapra CTM single screw extruder. The screw speed was about 40 rpm and the temperature profile from hopper to die: 90/160/160/160 °C.

Differential scanning calorimetry (DSC) data were collected on a Perkin Elmer DSC 7 instrument. Temperature scanning experiments were conducted as follows. Samples (10.0 ± 0.5 mg) were placed in open aluminum pans and heated from 25 to 300 °C at scan rates of 2, 5, 10 and 20 °C/min in air flowing at 50 mL/min. Based on the outcome of these results, suitable temperatures were chosen for the isothermal runs. The variability in the OIT values were studied using multiple repeat runs for each antioxidant at the 0.38% level. For OIT, the fastest possible heating rate was applied to reach the required isothermal temperature. After a 5 min soak time at this temperature, the purge gas was changed from nitrogen to air, where after the run was continued at the isothermal temperature for 60 min.

Data reduction proceeded as follows: The activation energies applicable to the isothermal experiments were obtained using linear least squares regression with the logarithmic form of Eq. 5. A similar procedure was followed for the dynamic data. In this instance the activation energy (E) was a priori assumed constant for a given antioxidant irrespective of its concentration. Thus a global activation energy value E value was obtained using a linear least squares data fit of Eq. 15. The intercept K_i values were allowed to vary with antioxidant concentration. From these estimates were obtained for the τ values as a function of antioxidant type and concentration. The overall results are summarized in Table 3.

Table 3 Summary of regression results obtained in an air atmosphere

	Concentration	wt%	0.05	0.10	0.20	0.38	0.74
	Antioxidant	$E/\text{kJ mol}^{-1}$	τ/fs	τ/fs	τ/fs	τ/fs	τ/fs
OOT	Anox 20	179 ± 6			0.197	0.364	0.658
	Naugard P	128 ± 8			5132	6850	8366
	Orox PK	160 ± 8	53.4	70.6	109	102	114
	Virgin	122	6800				
OIT	Anox 20	205 ± 14				0.00036	
	Naugard P	160 ± 7				1.85	

Results and discussion

Figure 3 compares typical isothermal scans obtained in this investigation. The scan obtained at 225 °C for the 0.20 wt% Anox 20 sample shows the expected precipitous decrease in the heat flux at ca. 15 min. However, the trace for the 0.38 wt% Orox PK sample obtained at 195 °C shows only a gradual decrease over a wider temperature range. All the Orox PK-containing samples showed this anomalous behavior. It was therefore not possible to determine consistent OIT values for this additive as a distinctive onset temperature could not be made out. Changing the oxidizing atmosphere from air to oxygen did not improve matters either. As a result, further isothermal analysis was limited here to the other two antioxidants. In contrast, no such problems were experienced using dynamic temperature scanning. This is illustrated by the traces shown in Fig. 4 for Orox PK. They provide clear evidence for the onset of an oxidation reaction at temperatures of ca. 227 and 236 °C, respectively.

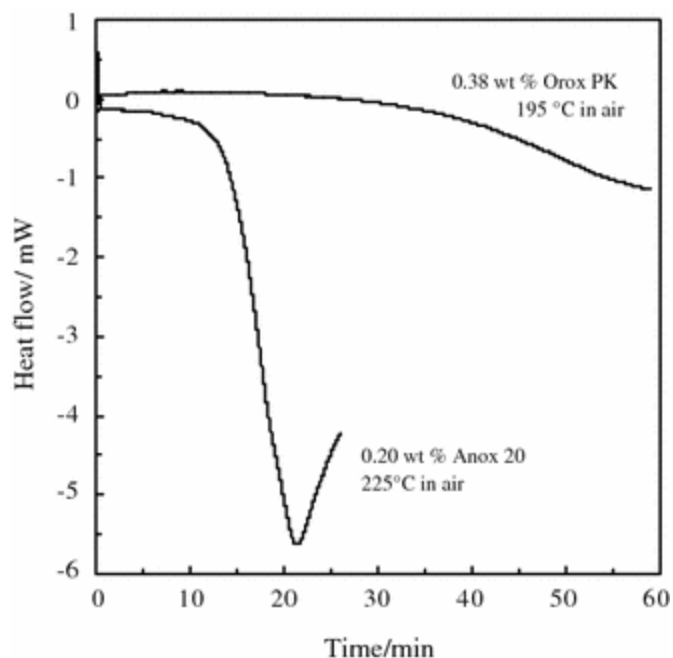


Fig. 3 Isothermal DSC scans obtained for two different stabilizers using air as atmosphere

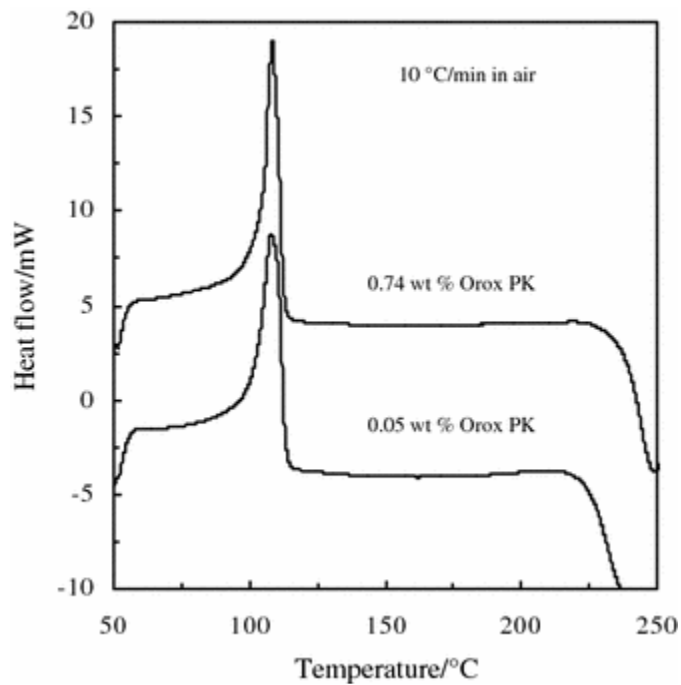


Fig. 4 Dynamic DSC scans for two samples containing different levels of Orox PK as stabilizer

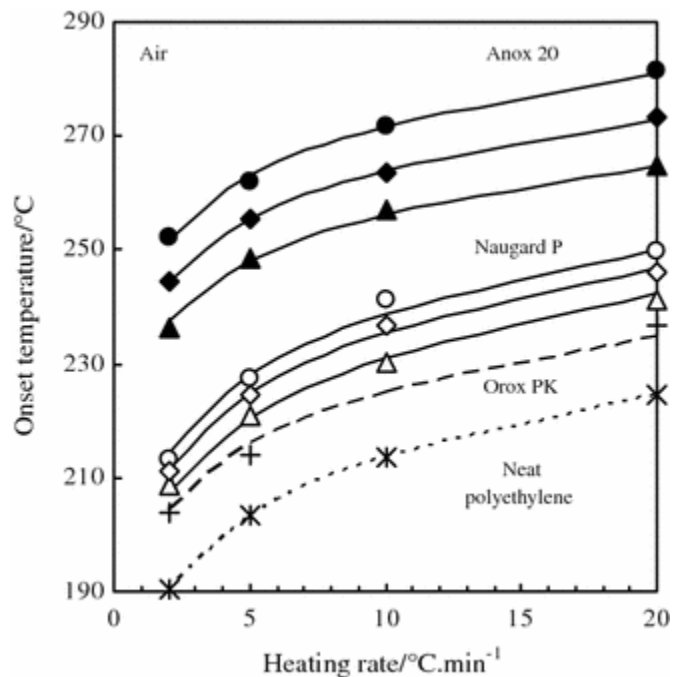


Fig. 5 Dynamic DSC data obtained using air as atmosphere. The symbols represent actual experimental data points whereas the solid lines represent the fit obtained with Eq. 15. Key: *asterisk* virgin polymer; *plus* 0.05 wt% Orox PK; *open triangle* 0.20, *open diamond* 0.38, *open circle* 0.74 wt% Naugard P; *filled triangle* 0.20, *filled diamond* 0.38, *filled circle* 0.74 wt% Anox 20

Figure 5 shows that OOT values increase with temperature scan rate and antioxidant concentration. The measured onset temperatures were highest for the phenolic antioxidant followed by the phosphite and then the aromatic amine. As expected the OOT values were lowest for the neat polyethylene. The difference between the OOT values recorded for samples containing 0.2 to 0.74 wt% Orox PK samples agreed to within experimental error. This suggests that the solubility limit of this additive in the molten polyethylene may have been exceeded at these high antioxidant concentrations.

Figure 6 shows the linear regression fits obtained by using Eq. 15 with $c = 1.894661$. This figure actually plots $K_i - \ln(b/T^c)$ as the ordinate value. This off-setting was done to aid the visualization of the overall data trends. Note that the K_i are the intercept values generated by linear regression of the individual data sets comprising OOT values obtained at different scan rates for a given antioxidant at a fixed concentration. The good fits shown in Fig. 6 validate the assumption of concentration-independent activation energies: All the experimental data for each antioxidant are adequately described by a single line with a fixed slope. The root mean square deviations, between experimental and predicted values, were less than 1.1 °C in all cases and the maximum deviation was 2.3 °C.

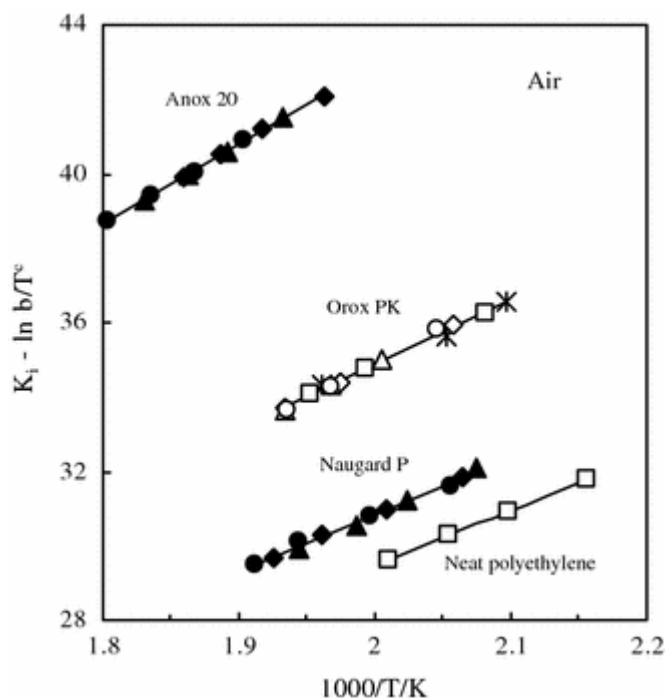


Fig. 6 Dynamic DSC data linear regression plots. The symbols represent actual experimental data points whereas the solid lines represent the fit obtained with Eq. 15. Key: *plus* 0, *asterisk* 0.05, *open square* 0.10, *open triangle* or *filled triangle* 0.20, *open diamond* or *filled diamond* 0.38, *open circle* or *filled circle* 0.74 wt% antioxidant

Figure 7 shows a plot of the characteristic time constant τ against antioxidant concentration. For Orox PK, τ approaches a limiting value of ca. 110 fs at concentrations above 0.20 wt%. Plateau values may indicate that a solubility limit of the antioxidant in the polyethylene matrix may have been reached or exceeded. Eq. 6 indicates that a slope of unity in Fig. 7 implies that zero order depletion kinetics, i.e. a direct proportionality between the time constant τ and the antioxidant

concentration. In the case of Anox 20 the slope equals 0.92, i.e. somewhat lower than unity. For Naugard P and the lower concentrations of Orox PK, the slopes are significantly lower equaling 0.37 and 0.51, respectively. The corresponding reaction orders are 0.63 and 0.49. These observations are at odds with the findings of Shlyapnikov and Tyuleneva [8]. They found that the antioxidant depletion during the induction period follows first order kinetics. In this case the concentration dependence of τ should obey Eq. 7 but this was not the case. Clear conclusions cannot be made in this regard in view of the limited number of inhibitor concentrations that were tested and the fact that we used an apparent rate equation that does not necessarily allow for a realistic mechanistic interpretation.

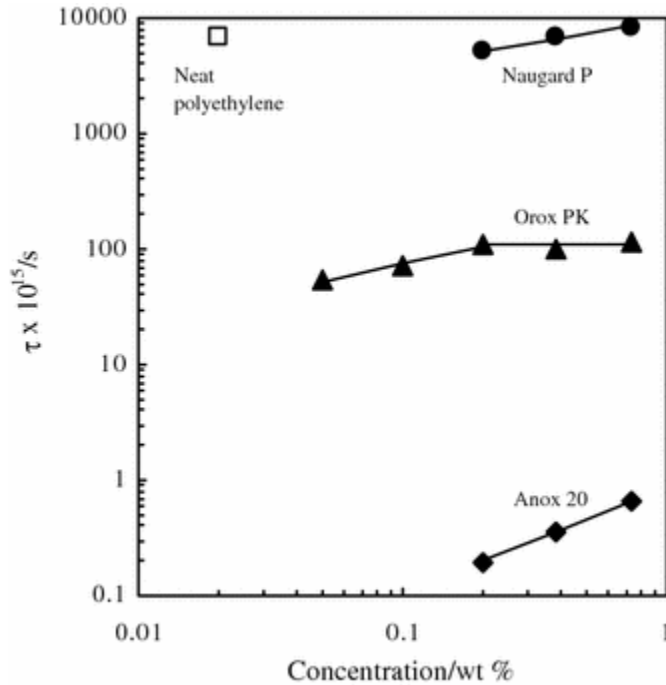


Fig. 7 The dependence of τ on antioxidant concentration calculated from OOT data

Figure 8 shows OIT data obtained in air at the 0.38% dosage level for Anox 20 and Naugard P, respectively. As mentioned earlier, it was not possible to extract sensible OIT values from all the isothermal runs conducted with Orox PK. Thus further analysis was limited here to the other two antioxidants. Direct linear regression reveals that OIT data for the other two antioxidants does conform to the trend predicted by Eq. 5 for the isothermal condition. Figure 8 also shows the experimental OOT values obtained at the same antioxidant concentrations. An important point to note here is that the measured OOT temperatures are a good deal higher than the isothermal temperatures which varied from 185 to 237 °C. Polyethylene processing temperatures range from as low as 160 °C for film blowing to as high as 310 °C in melt coating operations. The highest OOT recorded in this study was 281.3 °C, still well inside the range of actual processing temperatures.

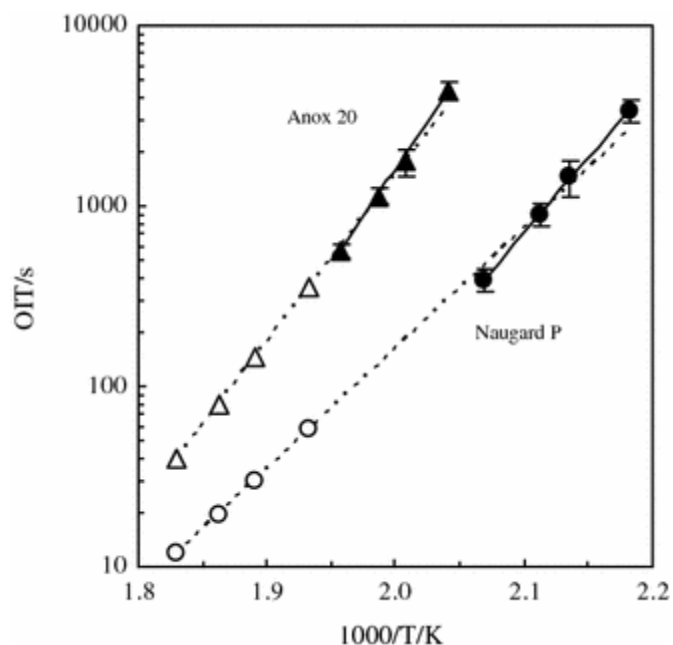


Fig. 8 Isothermal data (OIT) data (*solid symbols*) obtained in air for Anox 20 and Naugard P at the 0.38 wt% dosage level. The *open symbols* indicate measured OOT's and the *broken lines* the dynamic data fit. The *solid lines* represent the best fits of Eq. 12 to the isothermal data

The trend predicted for OIT from the OOT data through Eqs. 12, 14 and 16 is also shown in Fig. 8. This line dissects the row of OIT data points but clearly has a lower slope than the best isothermal line determined using the logarithmic form of Eq. 5. Table 3 also reveals that the 95% confidence intervals determined for the respective activation energies do not overlap. The implication is that the difference in the slopes determined using the isothermal and dynamic data is statistically significant. This is not entirely unexpected. The “single step reaction” model considered here is a gross oversimplification of the actual situation comprising numerous interacting reactions. These have different activation energies and, as a result, changing temperature changes their relative importance. This is experienced in the “single step approximation” as a temperature-dependent activation energy. It should also be mentioned that the assumption of an Arrhenius-type temperature dependence for the single-step approximation may actually be unrealistic [36].

The present results thus indicate that the OOT and OIT data belong to two different single-step approximations valid for separate and widely differing temperature regimes. Despite this fact, the deviations between OOT predicted and experimental OIT values are not excessive. The maximum and average absolute deviations were 18% and 7% for the Anox 20 samples and 22% and 14% for the Naugard samples. The reason for this can be found in the fact that the regression lines developed from the respective data sets dissected each other in the range of OIT measurement temperatures.

Conclusions

The effect of three different antioxidants, on the thermo-oxidative stability of a low density polyethylene melt, was valuated in air using DSC. OIT and OOT were determined at different

isothermal conditions and temperature scan rates, respectively. The experimental results were analyzed in terms of the single-step kinetics approximation. The main advantage of this description is that it enables a simple mathematical description because the temperature and conversion functions are separable. However, the price paid for this is a definite loss of insight into the actual stabilizing mechanism.

In contrast to the widely or tacitly accepted Gimzewski postulate, we proposed that the antioxidant depletion reaction constitutes the rate limiting process defining the length of the induction period. In this case catastrophic polymer degradation commences only once exhaustion of the antioxidants occurs. This defines the end of the induction period for both the isothermal and the dynamic experiments. Since the conversion at this point is effectively fixed at a value approaching unity, the OIT and OOT data can be treated according to the established isoconversion methods of thermal analysis. Both the isothermal and dynamic processes can then be described by a time constant that is characteristic of the antioxidant depletion reaction. An advantage of the present proposal is that this time constant can be related to the initial antioxidant concentration provided the conversion function is known.

Equation 12 succinctly defines the dimensionless link between OIT (t_{iso}) and OOT (T_{onset}). The present OIT data showed the expected Arrhenius-type temperature dependence predicted by this relationship. The Muduhusanan–Tang approximation for the temperature integral also allows one to obtain the activation energy from a straight line plot using OOT data in appropriately recast format as indicated by Eq. 15. Good linear regression fits were obtained with the present OOT data. It was found that the activation energy (E), while unique for each individual antioxidant, can be assumed independent of its initial concentration.

The revised Gimzewski model was tested by attempting to predict OIT values from OOT generated model parameters. The deviations between predicted and experimental data were similar in magnitude than the inherent scatter in the isothermal data. However, regression of the dynamic OOT data yielded significantly lower activation energy values than were obtained by direct regression of isothermal (OIT) data. This difference was found to be statistically significant. The discrepancy can possibly be attributed to the fact that the OIT and OOT data are obtained at very different temperatures.

A remarkable observation was the impossibility of obtaining reliable OIT values for Orox PK as antioxidant. Despite this shortcoming, quite acceptable OOT values could be found. Clearly, in such instances OOT offers a distinct advantage over the more established OIT quality control technique.

Acknowledgements Financial support for this research, from the Institutional Research Development Programme (IRDP) and the THRIP program of the Department of Trade and Industry and the National Research Foundation of South Africa as well as Xyris Technology CC, is gratefully acknowledged.

References

1. Bolland JL, Gee G. Kinetic studies in the chemistry of rubber and related materials. II. The effect of oxidation of unconjugated olefins. *Trans Faraday Soc.* 1946;42:236–43.
2. Colin X, Verdu J. Polymer degradation during processing. *C R Chimie.* 2006;9:1380–95.
3. Al-Malaika S. Perspectives in stabilisation of polyolefins. *Adv Polym Sci.* 2004;169:121–50.
4. Malík J, Kröhnke C. Polymer stabilization: present status and possible future trends. *C R Chimie.* 2006;9:1330–7.
5. Gömöry I, Čech K. A new method for measuring the induction period of the oxidation of polymers. *J Thermal Anal.* 1971;3:57–62.
6. Gimzewski E. The relationship between oxidation induction temperatures and times for petroleum products. *Thermochim Acta.* 1992;198:133–40.
7. Šimon P, Kolman L. DSC study of oxidation induction periods. *J Thermal Anal Calorim.* 2001;64:813–20.
8. Shlyapnikov YA, Tyuleneva NK. Inhibited oxidation of polyethylene: anatomy of induction period. *Polym Degrad Stab.* 1997;56:311–5.
9. Pospíšil J, Horák Z, Pilař J, Billingham NC, Zweifel H, Nešpůrek S. Influence of testing conditions on the performance and durability of polymer stabilisers in thermal oxidation. *Polym Degrad Stab.* 2003;82:145–62.
10. Koutný M, Václavková T, Matisová-Rychlá L, Rychlá J. Characterization of oxidation progress by chemiluminescence: a study of polyethylene with pro-oxidant additives. *Polym Degrad Stab.* 2008;93:1515–9.
11. Brown GP, Haarr DT, Metlay M. The use of thermal analysis methods for the estimation of thermal life ratings of magnet wire enamels. *IEEE Trans Electric Insulat.* 1973;EI-8:36–41.
12. Gedde UW, Jansson J-F. Determination of thermal oxidation of high density polyethylene pipes using differential scanning calorimetry. *Polym Test.* 1980;1:303–12.
13. Budrugaec P. Lifetime prediction for polymers via the temperature of initial decomposition. *J Thermal Anal Calorim.* 2001;65:309–12.

14. Mason LR, Reynolds AB. Standardization of oxidation induction time testing used in life assessment of polymeric electric cables. *J Appl Polym Sci.* 1997;66:1691–702.
15. Mason LR, Reynolds AB. Comparison of oxidation induction time measurements with values derived from oxidation induction temperature measurements for EPDM and XLPE polymers. *Polym Eng Sci.* 1998;38:1149–53.
16. Schmid M, Ritter A, Affolter S. Determination of oxidation induction time and temperature by DSC. Results of round robin test. *J Thermal Anal Calorim.* 2006;83:367–71.
17. Blaine RL, Lundgren CJ, Harris MB. Oxidative induction time – a review of DSC experimental effects. *ASTM STP 1326* (1997).
18. Blaine RL, Riga AT. Recertification of the polyethylene oxidation induction time reference material. *Thermochim Acta.* 2003;399:209–12.
19. Goh SH. Further study on the prediction of isothermal induction time by dynamic differential scanning calorimetry. *Thermochim Acta.* 1984;80:75–80.
20. Goh SH. Thermoanalytical studies of rubber oxidation: correlation of activation energy, isothermal induction time and oxidation peak temperature. *Thermochim Acta.* 1984;77:275–80.
21. Šimon P. Induction periods. *J Thermal Anal Calorim.* 2006;84:263–70.
22. Madhusudanan PM, Krishnan K, Ninan KN. A new approximation for the $p(x)$ function in the evaluation of non-isothermal kinetic data. *Thermochim Acta.* 1986;97:189–201.
23. Gugumus F. Re-examination of the thermal oxidation reactions of polymers 2. Thermal oxidation of polyethylene. *Polym Degrad Stab.* 2002;76:329–40.
24. Gugumus F. Re-examination of the thermal oxidation reactions of polymers 3. Various reactions in polyethylene and polypropylene. *Polym Degrad Stab.* 2002;77:147–55.
25. Boersma A. Predicting the efficiency of antioxidants in polymers. *Polym Degrad Stab.* 2006;91:472–8.
26. Colin X, Audouin L, Verdu J. Determination of thermal oxidation rate constants by an inverse method. Application to polyethylene. *Polym Degrad Stab.* 2004;86:309–21.
27. Šimon P. Considerations on the single-step kinetics approximation. *J Thermal Anal Calorim.*

2005;82:651–7.

28. Anderson HL, Kemmler A, Hohne GWH, Heldt K, Strey R. Round Robin tests on the kinetic evaluation of a solid-state reaction from 13 European laboratories. Part 1. Kinetic TG-analysis. *Thermochim Acta*. 1999;322:33–53.
29. Galwey AK, Brown ME. Application of the Arrhenius equation to solid state kinetics: can this be justified? *Thermochim Acta*. 2002;386:91–8.
30. Starink MJ. The determination of activation energy from linear heating rate experiments: a comparison of the accuracy of isoconversion methods. *Thermochim Acta*. 2003;404:163–76.
31. Flynn JH. The ‘Temperature Integral’ – its use and abuse. *Thermochim Acta*. 1997;300:83–92.
32. Ji LQ. New rational fraction approximating formulas for the temperature integral. *J Thermal Anal Calorim*. 2008;91:885–9.
33. Focke WW, Smit MS, Tolmay AT, van der Walt LS, van Wyk WL. Differential scanning calorimetry analysis of thermoset cure kinetics: phenolic resole resin. *Polym Eng Sci*. 1991;31:1665–85.
34. Tang W, Liu Y, Zhang H, Wang C. New approximate formula for Arrhenius temperature integral. *Thermochim Acta*. 2003;408:39–43.
35. Flynn JH, Wall LA. A quick, direct method for the determination of activation energy from thermogravimetric data. *Polym Lett*. 1966;4:323–8.
36. Simon P, Hynek D, Malíková M, Cibulková Z. Extrapolation of accelerated thermooxidative tests to lower temperatures applying non-Arrhenius temperature functions. *J Thermal Anal Calorim*. 2008;93:817–21.